Available online at www.sciencedirect.com
SCIENCE DIRECT®
Polymer 45 (2004) 3961–3966
polymer
www.elsevier.com/locate/polymer

Structural and dynamic heterogeneity in a telechelic polymer solution

Dmitry Bedrov[a,*], Grant Smith[a], Jack F. Douglas[b]

[a]*Department of Materials Science and Engineering, University of Utah, 122 South Central Campus Drive, Room 304, Salt Lake City, UT 84112-0560, USA*

[b]*Polymers Division, National Institute of Standards and Technology, Gaithersburg, MD 20899, USA*

Received 23 July 2003; received in revised form 8 January 2004; accepted 8 January 2004

Abstract

We utilize molecular dynamics simulations to investigate the implications of micelle formation on structural relaxation and polymer bead displacement dynamics in a model telechelic polymer solution. The transient structural heterogeneity associated with incipient micelle formation is found to lead to a 'caging' of the telechelic chain end-groups within dynamic clusters on times shorter than the structural relaxation time governing the cluster (micelle) lifetime. This dynamical regime is followed by ordinary diffusion on spatial scales larger than the inter-micelle separation at long times. As with associating polymers, glass-forming liquids and other complex heterogeneous fluids, the structural τ_s relaxation time increases sharply upon a lowering temperature T, but the usual measures of dynamic heterogeneity in glass-forming liquids (non-Gaussian parameter $\alpha_2(t)$, product of diffusion coefficient D and shear viscosity η, non-Arrhenius T-dependence of τ_s) all indicate a *return to homogeneity* at low T that is not normally observed in simulations of these other complex fluids. The greatest increase in dynamic heterogeneity is found on a length scale that lies intermediate to the micellar radius of gyration and intermicellar spacing. We suggest that the limited size of the clusters that form in our (low concentration) system limit the relaxation time growth and thus allows the fluid to remain in equilibrium at low T.

Keywords: Intermicellar spacing; Telechelic solution; Homogeneous fluid

1. Introduction

There have been many recent experimental and computational studies indicating the existence of 'dynamic heterogeneity' in polymeric and other glass-forming liquids [1]. Recent molecular dynamics (MD) simulation studies [2–5] have further expounded upon the important role of dynamic heterogeneity (defined below) in governing relaxation behavior in polymer melts as the temperature is reduced toward T_g. Experimental and MD simulations studies of polymer dynamics at attractive interfaces [6–9] have shown that the dynamics of polymers new interfaces can be significantly slowed down and that this slowing down of polymer dynamics is accompanied by an increasing dynamic heterogeneity even at temperatures (T) much higher than T_g [6]. Dynamic heterogeneity has been also reported in associating polymer solutions that form thermoreversible gels [10]. Evidently, dynamic heterogeneity is not restricted to glass-forming liquids and it is interesting to inquire if, how and why it is exhibited in other 'complex' fluids.

Dynamic heterogeneity is a phenomenon that can arise in both the spatial and time domains and is recognizable by deviations from the properties of 'homogeneous' solutions and fluids. In idealized homogeneous fluids, the distribution of dynamical events approach simple limiting forms governed by the independence of successive dynamical events and by the finiteness of the averages and variances of the times separating these events. For example, the distribution of waiting times between conformational transitions in a polymer at high temperatures is expected to be Poissonian [11–14] because the transition events are described by an independent random process with finite variance and mean time. Upon lowering T towards the glass transition of the polymer melt, the conformational transitions become increasingly intermittent and conformational transition distribution become distinctly *non-Poissonian*. [11,12,15] Similarly, the deviation of the distribution of atom displacements from a Gaussian distribution (or

* Corresponding author. Tel.: +1-801-585-3949; fax: +1-801-581-4816.
E-mail address: bedrov@tacitus.mse.utah.edu (D. Bedrov).

0032-3861/$ - see front matter © 2004 Published by Elsevier Ltd.
doi:10.1016/j.polymer.2004.01.082

equivalently Brownian motion) is another indication of 'dynamic heterogeneity' that has been recognized in recent molecular dynamics simulations of glass-forming liquids upon cooling [16,17]. (The Gaussian distribution describes the limit distribution for a sum of a large number of independent random displacements whose variance and mean are finite). These deviations from 'homogeniety' in the liquid dynamics are often accompanied by *spatial dynamic heterogeneity* associated with spatial correlation of particles in a state of enhanced or diminished mobility relative to that expected from the distributions governing the homogeneous fluid state. Specifically, simulations on glass-forming liquids at low T have indicated the existence of particles that are relatively 'mobile' and 'immobile' with respect to Brownian motion and that these particles form increasingly large scale clusters upon cooling [18,19,20]. Evidence points to these clusters being the physical origin of the various measures of dynamic heterogeneity seen in experiments on glass-forming liquids. Notably, these structures are characterized by *both* structural heterogeneity and temporal intermittency in atomic displacements and have many impacts on fluid properties. One of the most symptomatic properties of this fluid condition is that the product of fluid shear viscosity (η) and translational diffusion coefficient (D) increases in the region where the heterogeneity becomes pronounced. The dynamically heterogeneous state is also characterized by the non-Gaussian parameter (α_2) involving 4th and 2nd moments of the particle displacement distribution function, defined such that $\alpha_2 = 0.0$ for Brownian motion. We consider these quantities below in characterizing dynamic heterogeneity in micelle-forming fluid.

While experiment and simulation have revealed increasing dynamic heterogeneity on cooling of polymer melts, dynamic heterogeneity in self-associating polymer solutions has been much less studied. In the present paper, we consider the nature of dynamic heterogeneity in a model self-associating polymer solution that cannot be classified either as a first order or second order phase transition, but where a well-defined thermodynamic [21] 'clustering transition' exists. Our molecular dynamics simulations of micelle-forming telechelic solution also exhibit dynamic heterogeneity, similar in many characteristics to previous simulations of glass-forming liquids [22] and the thermally reversible gelation of associating polymers [10]. However, we observe that once the micelles become well formed at low temperatures, the heterogeneity effects diminish. The limited spatial extent of the micelles apparently leads to limited change in the viscosity and structural relaxation time of the fluid in comparison with thermally reversible gelation and glass-formation. The aim of the present paper is to examine the relation between dynamic and spatial heterogeneity in a micelle-forming telechelic solution upon lowering temperature through the micellization transition and to relate this phenomena to previous observations of dynamic heterogeneity in other systems.

2. Simulation methodology

2.1. Molecular dynamics simulations

MD simulations were performed on an ensemble of bead-necklace telechelic polymers consisting of eight beads. All beads experience excluded volume interactions modeled by a shifted and truncated Lennard–Jones potential of the form,

$$U(r) = 4\varepsilon\left[\left(\frac{\sigma}{r}\right)^{12} - \left(\frac{\sigma}{r}\right)^{6}\right] + U(r_c) \quad r < r_c, r_c = 2^{1/6}\sigma \quad (1)$$

$$U(r) = 0 \quad r \geq r_c$$

with an (unshifted) Lennard–Jones well depth (ε) of 1/7. The bead diameter $\sigma = 1$ defines the unit length scale. End groups of each chain also had an additional attractive end-group/end-group interaction of unit magnitude $\varepsilon = 1$ (truncated at 2.5 σ). MD simulations were performed on an ensemble of 1000 chains at number bead density $\rho = 0.3$ in an *NVT* ensemble using the simulation package *Lucretius* [23]. No solvent molecules were explicitly present in the system. Simulations were performed over a range of temperatures $0.70 > T > 0.13$ (in reduced units) which spans the micellization temperature (see below). All properties reported below are expressed in terms of the energy and length scales, ε and σ, respectively [24].

2.2. Calculation of the dynamic structure factor

Structural relaxation in the model telechelic solution was monitored via the incoherent dynamic structure factor defined as,

$$I(q_0, t) = \frac{1}{N}\sum_{i=1}^{N}\frac{\sin q_0 R_i(t)}{q_0 R_i(t)} \quad (2)$$

where N is the number of end beads, q_0 is the magnitude of the scattering vector corresponding to the length scale on which motion of chain end-groups is maximum non-Gaussian (see discussion in Section 2) and $R_i(t)$ is the displacement of end-bead i after time t. The non-Gaussian character of bead displacements, can be quantified by the first non-Gaussian correction to $I(q_0, t)$ and is given by [25],

$$I(q_0, t) = I^{\text{Gauss}}(q_0, t)\left[1 + \frac{1}{2}\left(q_0^2\langle R(t)^2\rangle/6\right)^2\alpha_2(t) + \cdots\right] \quad (3)$$

where

$$I^{\text{Gauss}}(q_0, t) = \exp(-q_0^2\langle R(t)^2\rangle/6) = \exp(-q_0^2 D(t)t) \quad (4)$$

and

$$\alpha_2(t) = \frac{3\langle R(t)^4\rangle}{5\langle R(t)^2\rangle^2} - 1 \quad (5)$$

Here, $\langle R(t)^2\rangle$ is the mean-square displacement of end beads after time t and $D(t) = \langle R(t)^2\rangle/6t$ is the apparent diffusion

coefficient. Strongly non-Gaussian displacements can result in much slower structural relaxation [rate of decay of $I(q_0,t)$] compared to a material with the same intrinsic dynamics [i.e. the same $D(t)$] and Brownian particle displacements. The deviation of $\alpha_2(t)$ from zero is often taken as a measure of dynamic heterogeneity in glass-forming liquids and we consider this same quantity in the context of our telechelic solutions. By itself, $\alpha_2(t) \neq 0$ does not imply that the system is heterogeneous, but a non-zero $\alpha_2(t)$ is symptomatic at this condition. Further information (discussed below) is required to establish the correct interpretation of non-zero $\alpha_2(t)$ and identify the dynamic heterogeneity in any given system.

3. Results and discussion

3.1. Structure characterization

Fig. 1 shows the probability $P(m)$ of finding an end-group in a cluster of size m. We define an end-group to belong to a cluster if it is within a distance of 2.0 from any other end-group in the cluster. At all T investigated, we found extensive end-group clustering as well as geometric percolation as a consequence of polymer chains spanning the space between clusters [26]. For $T > 0.37$, $P(m)$ decreases monotonically with increasing cluster size. At these temperatures, while the majority of end-groups participate in relatively small clusters ($m < 20$), there is a significant probability for having relatively large clusters ($m > 50$) which are spatially diffuse and dynamically unstable. The weight averaged cluster radius of gyration (R_g) at these temperatures is about 3.4. Near $T = 0.37$, we observe the emergence of a shoulder in $P(m)$, which we take as T_x the onset temperature of micelle formation [26]. Below this T, the shoulder transforms into a pronounced peak. For $T < 0.37$, we find that the intermediate size ($m \sim 25$–35) clusters are spatially compact ($R_g = 1.6$) and dynamically stable. In Fig. 2, we show T-dependence of the averaged cluster radius of gyration. After the onset of micellization, we do not observe additional qualitative changes in $P(m)$ with a further reduction in temperature.

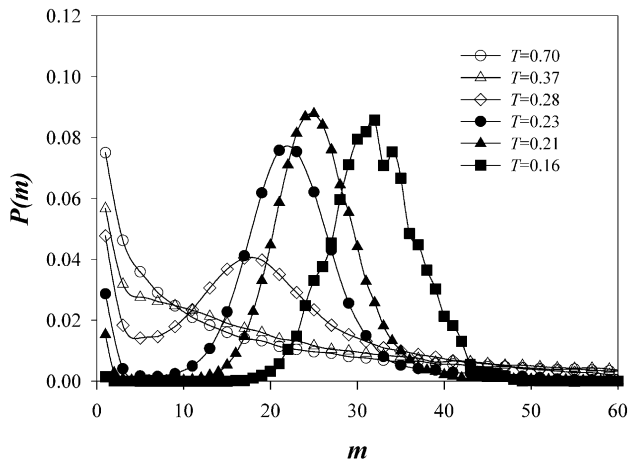

Fig. 1. The probability of finding an end-group in a cluster of size m for various T investigated.

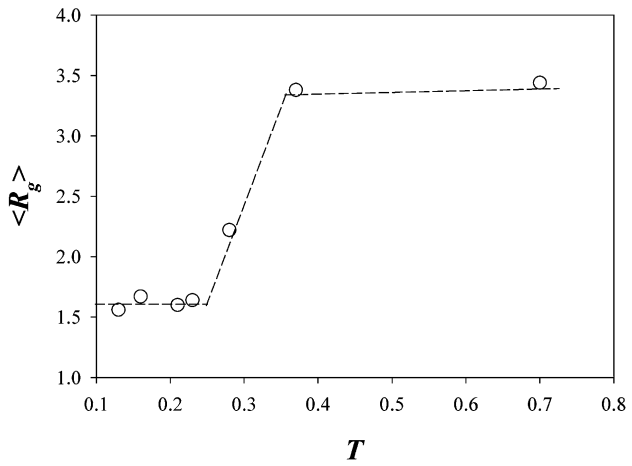

Fig. 2. Averaged cluster radius of gyration as a function of temperature.

Fig. 3 shows the center of mass distribution function for micelles of size greater than $m = 10$. With the emergence of well-defined clusters ($T < T_x$), an increase in liquid-like ordering of the micelles manifested through increasing nearest-neighbor peak intensity and the emergence of longer-range (second and third neighbor, etc. peaks) can be observed. The position of nearest neighbor peak ($r \approx 7.0$), however, is only weakly dependent on T.

3.2. Non-Gaussianity of end-group displacements

The second cumulant of the distribution of end-group displacements (Eq. (5)) is a measure of the extent of deviation of the end-group displacements from Gaussian behavior. The second cumulant (defining the non-Gaussianity parameter) is shown as a function of mean-square displacement of end-groups in Fig. 4. The maximum value of $\alpha_2(t)$

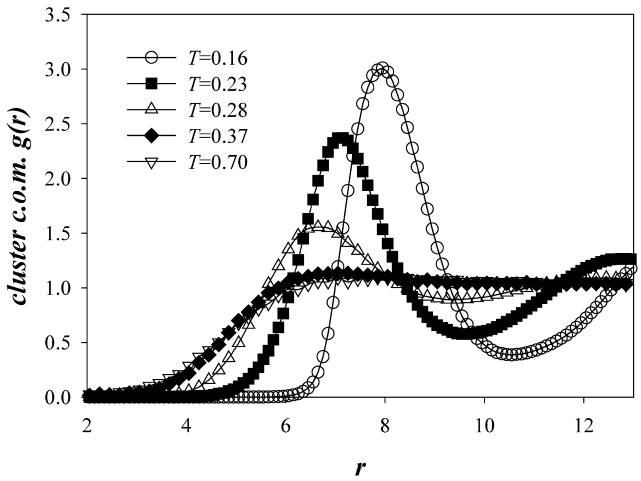

Fig. 3. The cluster center of mass radial distribution functions for clusters with $m \geq 10$.

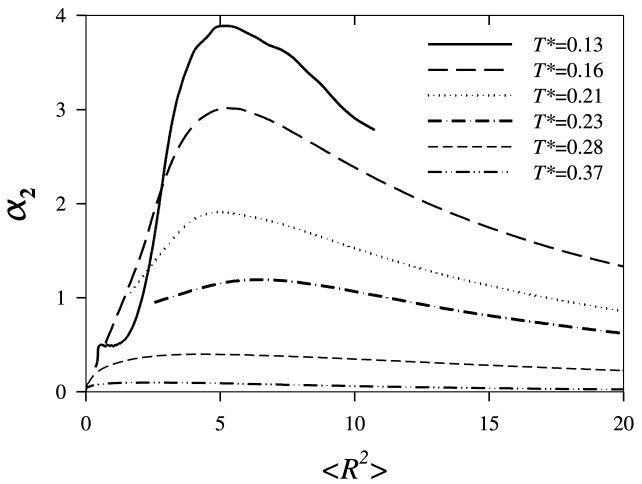

Fig. 4. $\alpha_2(t)$ as a function of mean-square displacement of end-groups.

increases with decreasing temperature for $T < T_x$, while the mean square displacement associated with this maximum remains essentially independent of temperature at $\langle R^2 \rangle = 5.3$. This defines a third length scale ($R(\alpha_2 - \max) = 2.3$) induced by the emergence of micelles and which can be thought of as a cage size [26]. This scale lies between the radius of gyration of the micelles ($R_g \approx 1.6$) and the mean intermicellar spacing ($R_{inter} \approx 7.0$).

3.3. Dynamic structure factor

The incoherent dynamic structure factor, calculated for end-groups only, is shown in Fig. 5 for T above and below the micellization temperature for $q_0 = 2\pi/R(\alpha_2 - \max) = 2.7$. The rate of decay of $I(q_0, t)$ decreases with decreasing temperature, indicating that the end-group dynamics, and hence structural relaxation, are slowing down appreciably. Also shown in Fig. 5 is the corresponding $I^{\text{Gauss}}(q_0, t)$, which reflects the intrinsic 'diffusion' of the end-groups (see Eq. (4)). The difference in the rate of decay between $I(q_0, t)$

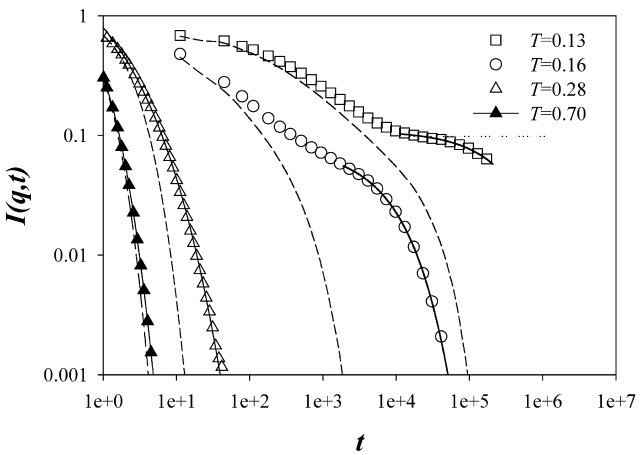

Fig. 5. The $I(q_0, t)$ (symbols) and $I^{\text{Gauss}}(q_0, t)$ dash lines as a function of t for $q_0 = 2.7$. Solid lines show the fits of terminal relaxation for $I(q_0, t)$ by KWW expression (Eq. (6)). Horizontal dotted line indicates a plateau value of $I(q_0, t)$ for the lowest T investigated.

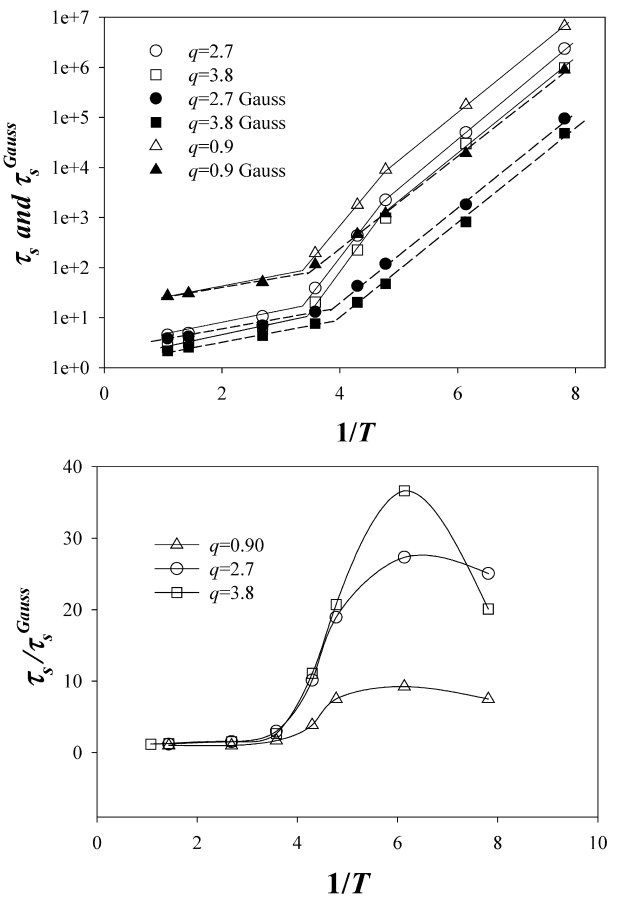

Fig. 6. Relaxation times τ_s, τ_s^{Gauss} (panel a) and the ratio $\tau_s/\tau_s^{\text{Gauss}}$ (panel b) are shown as a function of $1/T$ for three q_0 values corresponding to the length scales of R_g, $R(\alpha_2 = \max)$ and R_{inter}.

and $I^{\text{Gauss}}(q_0, t)$ at a given temperature is a manifestation of non-Gaussian end-group displacements, i.e. dynamic heterogeneity, on structural relaxation. It is clear that for T below the micellization temperature dynamic heterogeneity plays a much more important role in structural relaxation than for temperatures above T_x.

At low temperatures, the $I(q_0, t)$ shows a well-defined two-step relaxation with a clear plateau between steps as shown in Fig. 5 by a dotted horizontal line for $T = 0.13$. We define a structural relaxation time as a time when for a given q_0 value the $I(q_0, t)$ [or $I^{\text{Gauss}}(q_0, t)$] reaches a value of 0.01 of the plateau value for the lowest T investigated ($T = 0.13$). To obtain the structural relaxation time (τ_s) we fit the terminal relaxation process [$I(q_0, t)$ the below the second inflection point as indicated by solid lines in Fig. 4] using the Kohlrausch–Williams–Watts (KWW) equation, [27]

$$I(q_0, t) = A \exp[-(t/\tau)^{\beta}] \tag{6}$$

For $T = 0.13$ the constant A is equal to the plateau value of the $I(q_0, t)$ and therefore for all temperatures τ_s was determined by equating the KWW fit (r.h.s. Eq. (6)) to $0.01A_{T=0.13}$. The same procedure was used to determine $I^{\text{Gauss}}(q_0, t)$ relaxation times (τ_s^{Gauss}). In Fig. 6, the relaxation times τ_s, τ_s^{Gauss} and the ratio $\tau_s/\tau_s^{\text{Gauss}}$ are shown as a function

of inverse temperature. Data are shown for q_0 corresponding to the micelle radius of gyration, $R(\alpha_2 - \max)$, and the intermicellar spacing. On these length scales, the T-dependence of the τ_s, obtained from $I(q_0, t)$, increases dramatically for $T < T_x$ compared to $T > T_x$. This is consistent with the T-dependence of the shear relaxation time in the telechelic solution determined in our previous work [26]. It is interesting to point out that the shear stress modulus has a three-step relaxation at $T < T_x$ (not shown), while the structural relaxation exhibits two steps. The longest relaxation time in each type of the relaxation corresponds to the structural relaxation time and mean cluster lifetime, while the stress relaxation also exhibits a dependence on the 'caging time' characterizing the crossover from caged to diffusive motion in the mass diffusion.

Notably, the T-dependence of the structural relaxation time, determined from the mean-square displacements (τ_s^{Gauss}), is rather strong. Moreover, it can be well represented with two Arrhenius functions, and cannot be accurately represented with a Vogel–Fulcher [28] function commonly used to describe the temperature dependence of 'fragile' glass forming liquids, including polymers, approaching T_g. The latter fitting function predicts a diverging relaxation times with decreasing temperature, although it is unproven whether the relaxation times actually diverge in glass-forming liquids. The structural relaxation times for our telechelic solution, while showing a strong T-dependence below the micellization temperature, remain finite. The T-dependence of τ_s itself is more complex, apparently reflecting the T-dependence of the non-Gaussian contribution to structural relaxation (see below).

Fig. 6 also shows that the contribution of non-Gaussianity in end-group displacements to the structural relaxation time, quantified by $\tau_s/\tau_s^{\text{Gauss}}$, increases dramatically with decreasing T near T_x, the effect being greatest on the length scale of the maximum in α_2. This dramatic T-dependence of $\tau_s/\tau_s^{\text{Gauss}}$ persists only over a limited range of temperature below T_x. At lower T, the relaxation time ratio $\tau_s/\tau_s^{\text{Gauss}}$ saturates, leading to a complex T-dependence of τ_s.

3.4. Length and time scale dependence of dynamic heterogeneity

The maximum value of $\alpha_2(t)$ at each temperature, $\alpha_2^{\max}(T)$ is shown in Fig. 7 for the three length scales of interest (R_g, $R(\alpha_2 - \max)$, R_{inter}). The magnitude of $\alpha_2^{\max}(T)$ reaches a maximum near the micelle transition (maximum in specific heat [26]) and then decreases at lower T as the transition is 'completed', showing no tendency to diverge on any length scale. Furthermore, on longer length (time) scales, α_2 decreases dramatically for all T, indicating that the dynamics are rapidly homogenizing (i.e., displacements are becoming diffusive) on the longer length scale.

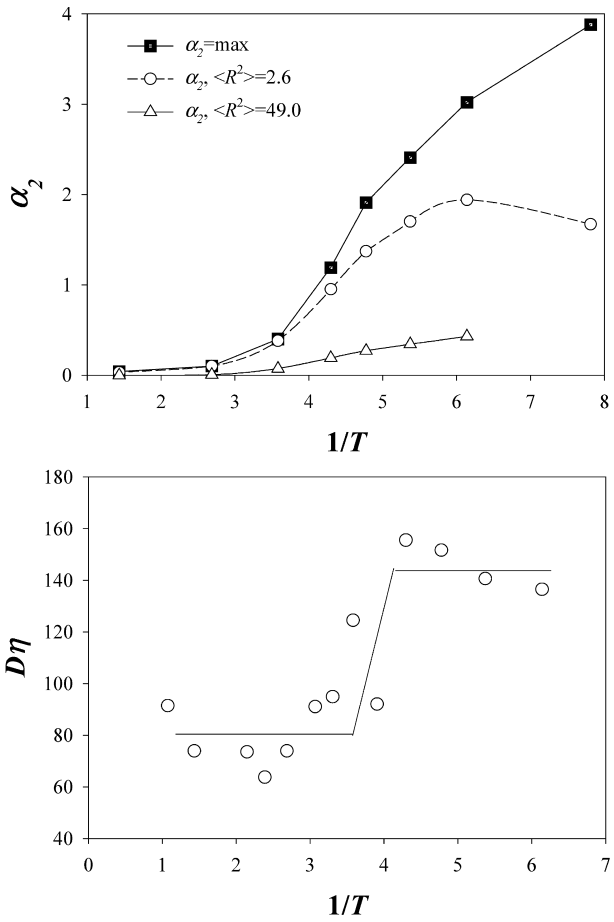

Fig. 7. (a) The maximum value of $\alpha_2(t)$ at each T, (b) the product of the molecular diffusion coefficient (D) and the solution viscosity (η).

This is consistent with the smaller $\tau_s/\tau_s^{\text{Gauss}}$ seen in Fig. 6 for the smallest q. We observe that the dynamic heterogeneity in our micelle-forming system has a clear origin in terms of the emerging structural heterogeneity (micelle formation) in the fluid.

Fig. 8 shows the probability distribution of end-group displacements for a mean-square displacement of $\langle R(t)^2 \rangle = 5.3$, corresponding to $\alpha_2^{\max}(T)$ for the telechelic solutions at several T. Also shown is the Gaussian distribution (corresponding to diffusive motion) for $\langle R(t)^2 \rangle = 5.3$ The heterogeneity in end-group dynamics that leads to increasingly large contributions of non-Gaussianity to the slowing structural relaxation with decreasing T can be clearly seen. At T below T_x, the displacement distribution is bimodal with relatively high probabilities for displacements at the scale of ≈ 1.3 and ≈ 7.0. The 1.3 scale corresponds to the R_g of the micelles and reflects the motion of end-groups still trapped within their micelle. The distance 7.0 is consistent with the nearest-neighbor intermicellar distance (see Fig. 2) and reflects the motion of end-groups that have 'jumped' to neighboring micelles. This jumping process leads to diffusive motion on larger length scales [26]. The maximum in $\alpha_2(t)$ occurs on a length (time) scale where the mean displacement of end-groups lies between these two scales

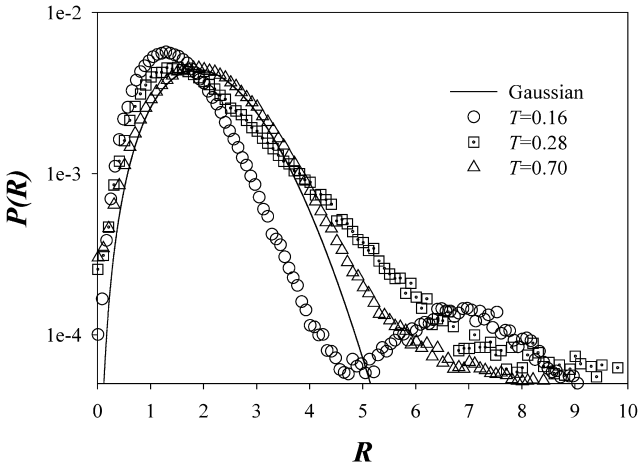

Fig. 8. The probability distribution of end-group displacements for a mean square displacement of $\langle R(t)^2\rangle = 5.3$, corresponding to $\alpha_2^{\max}(T)$, for the telechelic solutions at several T. Solid line corresponds to a Gaussian distribution with the same $\langle R^2\rangle$.

and thus reflects the fluid dynamic heterogeneity. Here, many end-groups are still trapped within their micelles, but many have also jumped, leading to quite non-Gaussian behavior in the displacement distribution. On longer length (time) scales, most end-groups have jumped, leading to more diffusive dynamics and a reduced dynamic heterogeneity.

The contrast in behavior of the telechelic solution and glass forming liquids is further illustrated by examining the T-dependence of the product of the molecular diffusion coefficient D and the solution viscosity η, shown in Fig. 7. This product is observed to strongly increase in 'fragile' glass-forming liquids as the glass transition is approached [1] and this is often taken as an indication of increasingly (spatially) heterogeneous dynamics. Fig. 7 reveals that while $D\eta$ increases as the T is decreased through T_x, this quantity saturates after a modest increase. This saturation of $D\eta$ parallels the change of relaxation time data from one Arrhenius regime at high T to another at low T, described above.

4. Conclusions

Detailed examination of structural relaxation in a model telechelic solution reveals a dramatic increase in the structural relaxation time as this solution pass below the micellization temperature. We also find substantial evidence for dynamic heterogeneity exhibited by the strong non-Gaussianity of bead displacements and an increase in the product $D\eta$. Although there are some qualitative similarities between dynamic heterogeneity of our micelle-forming solution with glass-forming fluids and thermoreversible gels, the extent of dynamic heterogeneity in our system is apparently much more limited at low T. Instead of a continually increasing dynamic heterogeneity with decreasing T, we find that it *saturates* at T below T_x for telechelic solution.

Acknowledgements

D.B. and G.D.S. were supported by the University of Utah Center for the Simulation of Accidental Fires and Explosions (C-SAFE), funded by the Department of Energy, Lawrence Livermore National Laboratory, under subcontract #B524196.

References

[1] Ediger MD. Annu Rev Phys Chem 2000;51:99.
[2] Smith GD, Borodin O, Paul W. J Chem Phys 2002;117:10350.
[3] Jin W, Boyd RH. Polymer 2002;43:503.
[4] Smith GD, Paul W, Monkenbusch M, Richter D. J Chem Phys 2001; 114:4285.
[5] Smith GD, Paul W, Bedrov D. In preparation.
[6] Smith GD, Bedrov D, Borodin O. Phys Rev Lett 2003;90:226103.
[7] Starr FW, Schroder TB, Glotzer SC. Phys Rev E 2001;64:021802.
[8] Forrest JA, Jones RAL. In: Karim A, Kumar S, editors. Polymer surfaces, interfaces and thin films. Singapore: World Scientific; 2000.
[9] Lin EK, Kolb R, Satija SK, Wu WL. Macromolecules 1999;32:3753.
[10] Kumar SK, Douglas JF. Phys Rev Lett 2001;87:188301.
[11] Smith GD, Borodin O, Paul W. J Chem Phys 2002;117:10350.
[12] Smith GD, Borodin O, Bedrov D, Paul W, Qiu XH, Ediger MD. Macromolecules 2001;34:5192.
[13] Borodin O, Smith GD. Macromolecules 2000;33:2273.
[14] Borodin O, Smith GD, Bandyopadhyaya R, Byutner O. Macromolecules, 2003;36:7873.
[15] Jin W, Boyd RH. Polymer 2002;43:503.
[16] Smith GD, Paul W, Monkenbusch M, Richter D. J Chem Phys 2001; 114:4285.
[17] Smith GD, Paul W, Bedrov D. In preparation.
[18] Ebremichael Y, Schroder TB, Satrr FW, Glotzer SC. Phys Rev E 2001;64:051503.
[19] Bennemann C, Donati C, Baschnagel J, Glotzer SC. Nature 1999;399: 246.
[20] Vollmayr-Lee K, Kob W, Binder K, Zippelius A. J Chem Phys 2002; 116:5158.
[21] Dudowicz J, Douglas JF, Freed KF. J Chem Phys 2000;112:1002.
[22] Bennemann C, Paul W, Binder K, Dunweg B. Phys Rev E 1998;57: 843.
[23] http://lucretius.mse.utah.edu.
[24] Allen MP, Tildesley DT. Computer simulation of liquids. New York: Oxford Press; 1987.
[25] van Megan W, Mortensen TC, Williams SR, Müller J. Phys Rev E 1998;58:6073.
[26] Bedrov D, Smith GD, Douglas JF. Europhys Lett 2002;59:384.
[27] Williams G, Watts DC. Trans Faraday Soc 1970;66:80.
[28] Strobl G. The physics of polymers. Concepts of understanding their structures and behavior. Berlin: Springer; 1997.